

Appropriate Acquisition and Processing for Shallow 3-D Seismic Surveys

Carlos E. Moreno*, Roger Adams Young, John P. Castagna,
The University of Oklahoma, Norman, OK

Summary

A conventionally processed, high-resolution 3-D seismic survey at the OU Gypsy test site exhibited poor ties to well control. The data was reprocessed with surface consistent predictive deconvolution, muting of wide-angle reflections, min/max exclusion stacking, and F-XY deconvolution. After reprocessing, a good character match with synthetic seismograms was observed.

Introduction

3-D seismic reflection surveys targeting features at depths of 1000 ft or less are commonly acquired nowadays. Many of these surveys are part of oil exploration or development programs by smaller energy industry companies and contractors, but the use of 3-D surveys outside the energy industry is also growing (eg., Vilella et al., 1997; Siahkoohi and West, 1998). The vast experience of the energy industry in acquisition and processing 3-D surveys provides a wealth of guidance for those less familiar with 3-D methods. However, relying on acquisition parameters and processing approaches designed for deeper targets may have its pitfalls. In the most unfavorable case, a survey may be both over-designed and unsuited for shallow imaging. A choice of processing parameters typical of deeper targets may also lead to a poor stack of shallow targets.

This paper shows how processing appropriate to shallow targets can produce a favorable image that greatly improves the tie with a zero-offset synthetic trace. It concludes with some suggestions about reprocessing the shallow reflections contained within data originally acquired with deeper objectives in mind.

Survey acquisition

Figure 1 shows the location of the Gypsy Project Subsurface study site NW of Tulsa, OK. This site was chosen by BP Petroleum for characterizing a clastic reservoir interval by borehole and surface geological and geophysical methods (Doyle and Sweet, 1995). A nearby outcrop study site afforded geological mapping and physical property measurements of the same units encountered at the subsurface site at a depth of approximately 1000 ft. The Gypsy database and the site itself were ceded to the University of Oklahoma by BP in 1994.

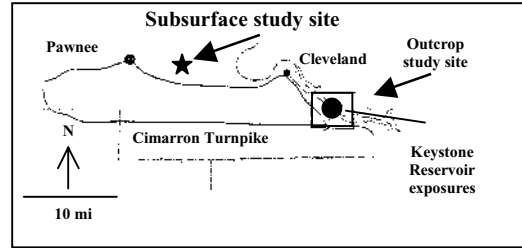


Figure 1 Location of the Gypsy study sites

The 3-D seismic survey at the Subsurface study site (Figure 2) was small in area, covering approximately 0.16 km² (40 acres).

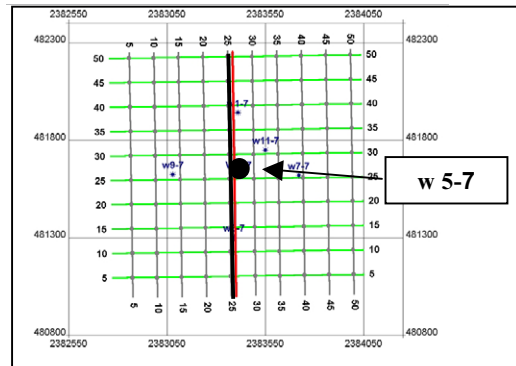


Figure 2 Survey basemap, inline 26, and well 5-7.

Recording parameters and acquisition geometry are given in Tables 1 and 2, respectively.

RECORDING	PARAMETERS
Recorded by	Western Geophysical
Date	Jan. 1990
Recording system	MDS-16
Format	SEG-B
Geophone type	LRS 1011 (28 Hz)
Filter	9-250 Hz
Notch filter	Out
Sample rate	1 ms
Record length	3000 ms
Bin size	25 ft by 25 ft

Table 1 Recording parameters for the 3-D survey

ACQUISITION	GEOMETRY
Energy source	Dynamite
Source pattern	Single charge (1 lb/shot)
	Shot depth 90, 100, 110, 120 ft (same hole, 3 times)
Shot interval	~140 ft
Number of shot lines	7 (45 deg to receivers)
Shot line separation	~250 ft
Shots per swath	40
Number of swaths	3
Receiver interval	50 ft (N-S)
Receiver line spacing	50 ft (E-W)
Receiver lines/shot	9 (every 150 ft)
Channels per rcv. line	27: 27x9=143 live ch/sht
Crossline line roll	1 receiver line (50 ft)
Inline line roll	0 (no movement N-S)
Geophones/station	12
Geophone array	25 ft circle

Table 2 Acquisition parameters for the 3-D survey

Standard Processing

The 3-D processing flow in this paper is chosen to image the shallow targets at times of 250 ms or less in the upper part of the data acquired. Two sequences of processing steps were applied to the 3-D data using ProMAX 3D. **Standard processing** (Table 3, top) included binning, amplitude recovery, trace editing, and statics correction. Nominal fold for inner bins exceeded 50, but the 70 % stretch mute limited the offset range in stacking very shallow events. Figure 3 shows that the effective fold for events at times less than 200 ms is approximately 10 or less. In the Gypsy interval at approximately 250 ms, however, the fold is nearly half the nominal fold. An upper datum was adopted, and residual statics was accomplished in a 3-D sense. Figure 4a shows inline 26 through residual statics.

STANDARD	PROCESSING
1.Geometry; binning	
2.True amp. recovery	a^{-z} , $a=1.5$
3.Trace editing	
4.Trace shortening	Reduce to 1 s
5. Datum statics correction	Final datum: 1000 ft
6. Resid. statics correction	
7. Resid. statics correction	
APPROPRIATE	PROCESSING
8. Bandpass filtering	35-45-250-400
9. Sur. con. pre. decon.	Op. Len.: 10 ms Win. Len.: 200 ms
10. NMO correction	Stretch mute: 70%
11. Angle-limited muting	Max. angle:~30 deg
12. Min/max excl stacking	
13. F-XY decon.	5 by 5 traces

Table 3 Processing steps

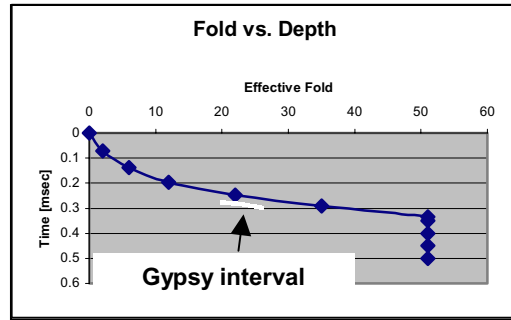


Figure 3 Fold decreases with depth due to the processing stretch mute.

Appropriate processing

Appropriate processing began with the result from standard processing and applied additional steps that take into account the special requirements of the shallow reflections. Table 3 (bottom) shows the steps in appropriate processing that were chosen after extensive parameter testing. These consist of bandpass filtering, surface consistent predictive deconvolution, angle-limited muting, minimum/maximum exclusion stacking, and F-XY deconvolution.

Bandpass filtering Figure 4b shows inline 26 through bandpass filtering (35-45-250-400). This filter is, essentially, a lowcut filter as spectra show that the highest frequency of the seismic data is less than 250 Hz. The improvement is due mainly to the attenuation of the groundroll, which has high-frequency modes that overlap the frequency band of reflections (Liu, 1999). The loss of reflection amplitude in this band is, of course, unfortunate and will affect the stack, but the improvement in S/N (Figure 4b, boxes) justifies the step.

Surface consistent predictive deconvolution Pre-stack surface consistent deconvolution not only increased noticeably the S/N ratio, it also improved the frequency bandwidth (Figure 4b and c, boxes), which would be important for a detailed interpretation.

Angle-limited mute Comparison of the synthetic trace (Figure 4, between panels) to the processing result through predictive deconvolution (Figure 4c) shows that there is a relatively good match between the two for times greater than 120 ms. It is clear, however, that the strongest events on the synthetic trace do not correspond to the strongest events in the stacked data. In particular, a strong, stacked event at approximately 185 ms (Figure 4c, arrow) does

not appear to have an equivalent on the synthetic trace. This lack of correspondence raises several questions. Is the log depth-to-time conversion inaccurate? Did the logging tool function properly? Is the seismic wavefield seeing the impedance changes shown by the sonic log?

An exhaustive analysis of the logs indicates that for a given depth the time difference is less than 6 ms suggesting that the depth-to-time curves are not the problem. Very careful editing of the logs has reduced the possibility of an anomalous impedance response. The presence of many events in the seismic data suggests that the seismic wavefield is, in fact, responding to impedance changes. This situation led us to question a fundamental assumption that is made in comparing the synthetic trace and the stacked section, namely, that the stacked trace is equivalent to a zero-offset trace. This may not be valid when data is stacked over a range of incidence angles because both amplitude and phase vary with angle. The result may be that the stacked event is not similar to the synthetic event.

In order to establish the range of incidence angles present in the binned gathers after stretch muting, CMP ray tracing was performed. These results were used to construct an angle-limited mute pattern. Figure 4d shows the stack after muting traces with angles of incidence exceeding approximately 30 deg. The stack corresponds much more favorably at 185 ms (Figure 4d, arrow) with the synthetic trace once the wide-angle reflections are eliminated from the stack.

Min/max exclusion stacking Both a mean stack and a non-conventional stack, the minimum/maximum exclusion method, were tested. The advantage of the latter is that it excludes anomalous values, and it drops null values due to muting. Figure 5 shows the two stacks after F-XY deconvolution. In order to equalize amplitudes, AGC was applied to gathers just before mean stack using a 1,000 ms window to preserve trace-to-trace amplitudes. Shallow events (solid box) are weaker than deeper events (dashed box) on the mean stack (Figure 5b, right) because muting is greater for shallower traces. The minimum/maximum exclusion method (Figure 5b, left), on the other hand, shows a much more uniform amplitude distribution for both shallow and deep events (Figure 5a: solid and dashed boxes, respectively).

F-XY deconvolution A final step, F-XY deconvolution, is applied in order to attenuate random noise remaining after stack.

Conclusions

3-D reflection processing requires additional steps to account for the special properties of shallow reflections. These steps may include bandpass filtering, predictive deconvolution, angle-limited muting, and min/max stacking, which take into account the overlap in signal and noise and the very wide range of incident angles at reflectors. A much better match between a zero-offset synthetic trace and the stacked section results if appropriate processing is used to attenuate residual groundroll, to improve the bandwidth of the data, to mute wide-angle reflections, and to drop from the stack null values resulting from muting.

When considering a reprocessing of 3-D data to enhance shallow reflections, a ray trace analysis using an approximate interval velocity model is important to establish the range of incidence angles expected for the shallow target horizons. Excluding the widest angles from the stack may be necessary to obtain a tie with well data.

Acknowledgments

The authors are grateful to the Gypsy Project, Institute for Reservoir Characterization, and the Institute for Exploration and Development Geosciences, Univ. of Oklahoma, for use of geophysical data, and to Bill Lamb for assistance in editing the log data. Financial support was provided by PDVSA and the OU Geophysical Reservoir Characterization Consortium.

References

- Villella, A. C., Xia, J. and Miller, R. D., 1997, Delineation of salt dissolution sinkholes using minimal deployment shallow 3-D seismic reflection surveying: Annual Meeting Abstracts, Society Of Exploration Geophysicists, 780-783.
- Siahkoohi, H. R. and West, G. F., 1998, 3-D seismic imaging of complex structures in glacial deposits: *Geophysics*, 63, no. 03, 1041-1052.
- Doyle, J.D., Sweet, M.L., 1995, Three-dimensional distribution of lithofacies, bounding surfaces, porosity, and permeability in a fluvial sandstone-Gypsy Sandstone of Northern Oklahoma, *AAPG Bulletin*, 70, 70-80.
- Liu, Z.-M., 1999, Methods of velocity determination and noise reduction in the processing of near-surface seismic reflection data, unpublished Ph.D. thesis, Univ. of Oklahoma, 186 pp.

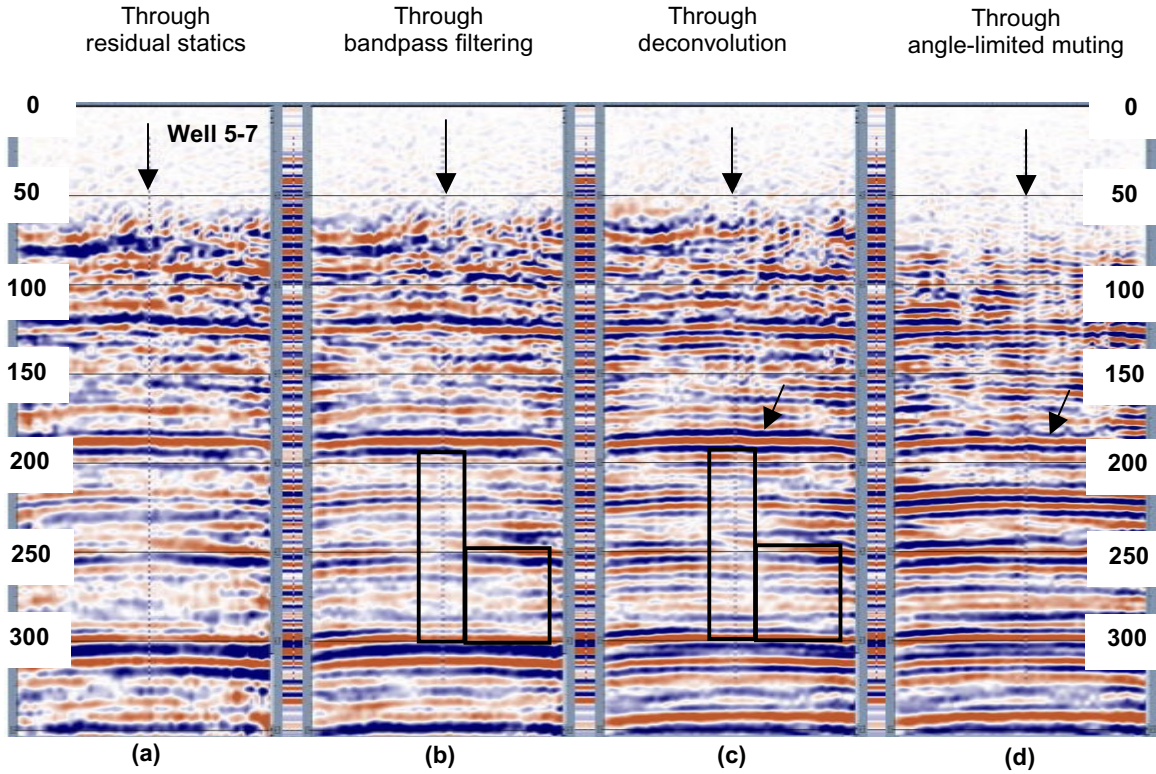


Figure 4 Processing stages: Standard processing (a). Appropriate processing (b-d). All sections are displayed with F-XY deconvolution. Small panels between sections are the zero-offset synthetic trace.

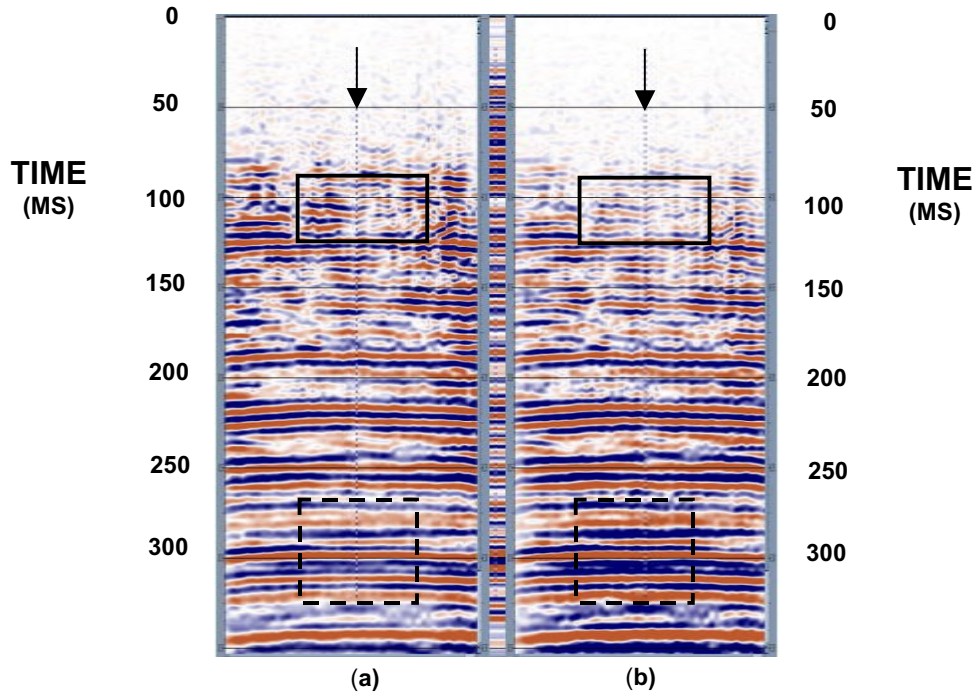


Figure 5 Stacking by (a) the minimum/maximum exclusion method; (b) the mean stack method. Both sections are displayed with F-XY deconvolution.